Broadband, polarization-insensitive, and wide-angle microwave absorber based on resistive film

Dan-Dan Bu(布丹丹), Chun-Sheng Yue(岳春生)†, Guang-Qiu Zhang(张广求), Yong-Tao Hu(胡永涛), and Sheng Dong(董胜)

National Digital Switching System Engineering & Technological R & D Center, Zhengzhou 450002, *China*

(Received 26 December 2015; revised manuscript received 8 March 2016; published online 25 May 2016)

A simple design of broadband metamaterial absorber (MA) based on resistive film is numerically presented in this paper. The unit cell of this absorber is composed of crossed rectangular rings-shaped resistive film, dielectric substrate, and continuous metal film. The simulated results indicate that the absorber obtains a 12.82-GHz-wide absorption from about 4.75 GHz to 17.57 GHz with absorptivity over 90% at normal incidence. Distribution of surface power loss density is illustrated to understand the intrinsic absorption mechanism of the structure. The proposed structure can work at wide polarization angles and wide angles of incidence for both transverse electric (TE) and transverse magnetic (TM) waves. Finally, the multi-reflection interference theory is involved to analyze and explain the broadband absorption mechanism at both normal and oblique incidence. Moreover, the polarization-insensitive feature is also investigated by using the interference model. It is seen that the simulated and calculated absorption rates agree fairly well with each other for the absorber.

Keywords: broadband, metamaterial absorber, resistive film, multi-reflection interference theory

PACS: 78.20.Ci, 42.25.Bs, 41.20.Jb **DOI:** 10.1088/1674-1056/25/6/067802

1. Introduction

The initial microwave absorber is Salisbury screen, which consists of the resistive layer surface, a quarter wavelength dielectric spacer, and the metal grounded plane.[1] As absorbing electromagnetic waves by thickness interference, Salisbury screen achieves the absorption of specific wavelengths of electromagnetic waves but obtains a narrow absorption band. Based on the absorbing mechanism of Salisbury screen, multilayer continuous resistive films and dielectric substrates arranged alternately with each other constitute Jaumann absorber.[2] In 2008, Landy *et al.* proposed the perfect metamaterial absorber (MA) first.[3] Subsequently, many MAs with new features were designed to achieve polarization-insensitive absorption[4–6] or wide-angle absorption.[7,8] However, most of these structures designed are based on strong electromagnetic resonance to effectively absorb the incident wave. Thus, the absorption bandwidths of these MAs are relatively narrow. In order to expand the absorption bandwidth, wideband MAs loaded lumped elements[9–11] have been proposed, but the cost is high and it is usually difficult to fabricate. Substituting the resistive pattern for the metallic structure, another class of MA is employed to implement broadband absorption,[12–14] which is easily processed and cost is low. For the theoretical analysis of absorbing properties of the MA, the generally accepted impedance matching principle can explain the absorption only qualitatively, while transmission line model[15,16] is only available in the case of normal incidence of electromagnetic waves with ignoring interaction between layers of absorbing structures. Compared with these two theoretical approaches, the interference theory[17–19] can not only quantitatively analyze the absorbing properties of MAs, but also quantitatively study the interaction between the internal metallic layers of the structures, meanwhile it is applicable to the complex structure under the oblique incidence condition. Previously, design and analysis of MAs using interference theory were focused on single-band and multi-band absorption.[20,21] Now, attention begins to shift to the study of wideband absorption of the MAs by using the interference theory. Chen *et al.* adopted first the interference model to explain the broadband absorption mechanism at both normal and oblique incidence.[14]

In this paper, we present a broadband, polarization-insensitive and wide-angle MA, which can be fabricated easily by traditional printed circuit board (PCB) technology and silk-screen printing.[14] The presented MA obtains wide frequency band absorption from 4.75 GHz to 17.57 GHz with absorption rate above 90%, and can achieve polarization-insensitive and wide-angle absorption for both TE and TM waves. The interference theory is used to explain the absorption mechanism at different angles of incidence and variable polarization angles.

2. Design and simulation

2.1. Absorption and distribution of power loss density

The proposed MA is designed and optimized by CST Microwave Studio based on the commercial finite difference time

†Corresponding author. E-mail: csyzhang@163.com

© 2016 Chinese Physical Society and IOP Publishing Ltd

domain (FDTD) solver. The schematic diagram and geometric parameters of the absorber unit cell are shown in Fig. 1. The substrate is modeled as polymethacrylimide (PMI) foam easily available from the market, with relative permittivity $\varepsilon_r \approx 1$ and relative permeability $\mu_r \approx 1$, whose thickness is set to be $t = 6$ mm. With electric conductivity $\sigma = 5.8 \times 10^7$ S/m, 0.035-mm-thick copper film is used on one side of the dielectric substrate while on the other side is the resistive film, whose pattern is of two crossed rectangular rings. Each of both the rectangle rings has the length $a = 15.5$ mm and its width is kept to be $b = 7.42$ mm. The lattice constant and the width of the resistive film are kept to be $p = 16$ mm and $w = 2$ mm, respectively. The surface resistance value of the resistive film is selected to be $R = 75$ Ω/sq. Because the thickness of copper film is much larger than the penetration depth of the incident wave, the transmission is zero for the whole frequency range and the reflectance is the only factor to determine the absorption. The absorption rate is characterized by $A(\omega) = 1 - R(\omega) = 1 - |S_{11}|^2$.[18]

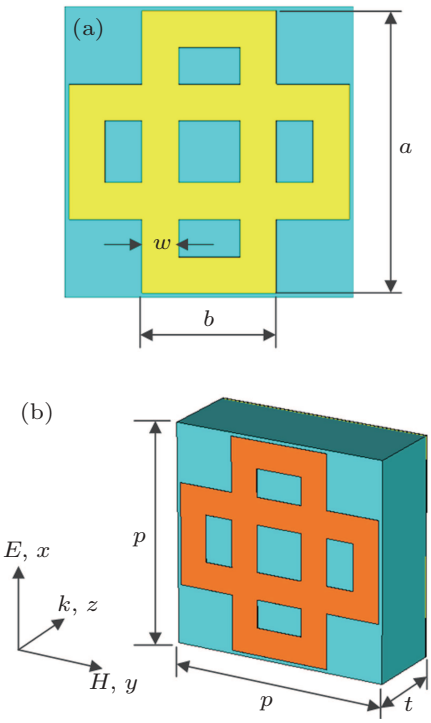


Fig. 1. (color online) Schematic diagram with geometric parameters of the broadband absorber unit cell. (a) The front view and (b) the perspective view.

The simulated reflectance, transmission and absorption spectra of the MA are shown in Fig. 2. The simulation results indicate that the designed structure obtains a 12.82-GHz-wide absorption from about 4.75 GHz to 17.57 GHz with absorptivity over 90% at normal incidence, while the transmission is always equal to zero at the whole frequencies of interest. It is indicated that the effective impedance of the absorber matches to free space and a large imaginary part of refraction index is achieved simultaneously in the wide frequency band range.

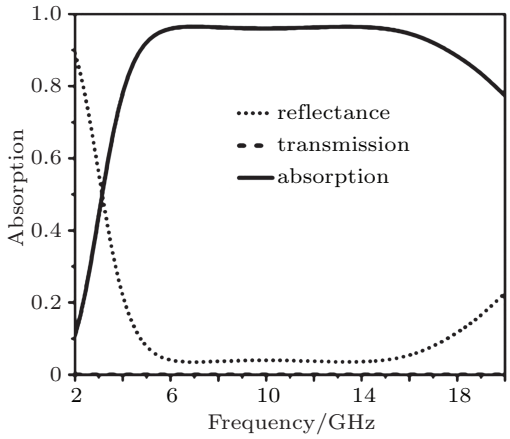


Fig. 2. Simulated reflectance (short dot curve), transmission (short dash curve), and absorption spectra (solid curve) of the absorber each as a function of frequency.

Considering the influences of substrate permittivity and width of the resistive film on the absorption of composite MA, we simulate the absorptivities of the MA with different substrate permittivities and widths of the resistive film as shown in Figs. 3(a) and 3(b), respectively. As shown in Fig. 3(a), with the increase of substrate permittivity ε_r, the high-frequency absorption bandwidth gradually decreases and the low-frequency high-absorptivity almost keeps unchanged. As shown in Fig. 3(b), the absorption bandwidth above 90% first increases and then decreases with the width of the resistive film w increasing.

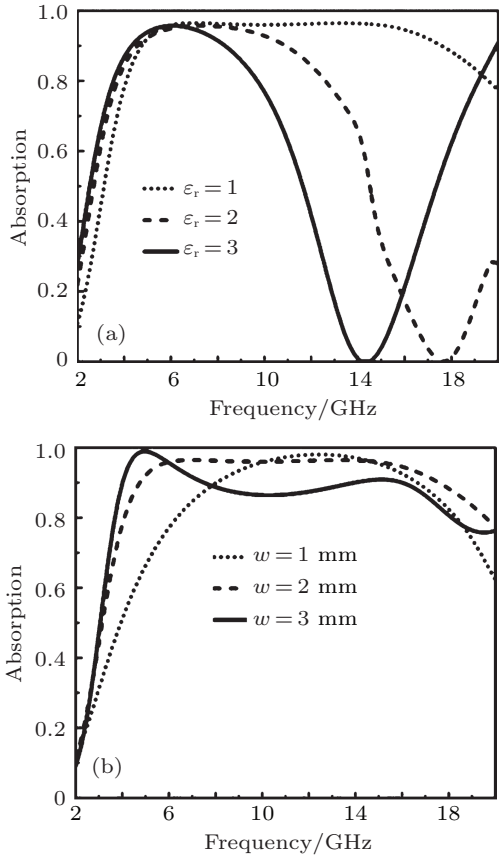


Fig. 3. Simulated absorption spectra of the absorbers with (a) different substrate permittivities and (b) different widths of the resistive film.

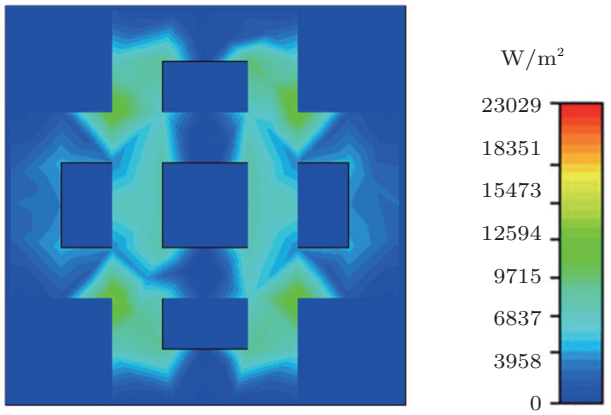


Fig. 4. (color online) Distribution of surface power loss density at 11 GHz of the proposed absorber.

To gain an insight into the intrinsic absorption mechanism, the distribution of power loss density at the midpoint 11 GHz of the whole frequencies of interest is given in Fig. 4. The result indicates that when the electric field direction is parallel to the axis ($E \parallel x$), the power loss mainly concentrates on one ring's two longer arms of the resistive film. Then, by combining with the absorbing feature of the designed structure, it is concluded that the crossed rectangular ring resistive film mainly supplies the broadband and high absorption due to the ohmic loss.

2.2. Polarization-insensitive and wide-angle absorption

The polarization-insensitive feature is characterized by setting the polarization angles from 0° to 80° in steps of 20° at normal incidence. Figures 5(a) and 5(b) indicate simulated absorption spectra each as a function of frequency and polarization angle for TE and TM waves, respectively. Clearly, as the polarization angle increases from 0° to 80°, the absorption spectra for TE and TM waves remain almost unchanged, which demonstrates that this absorber is polarization-insensitive under the normal incidence.

Next, the performances of the proposed absorber at various incident angles are investigated. The simulated absorption rates at different angles of incidence for TE and TM waves are depicted in Figs. 5(c) and 5(d), respectively. For the TE wave given in Fig. 5(c), the amplitude of absorption slightly decreases as the incident angle varies from 0° to 60°. Beyond 60°, the absorptivity and bandwidth decrease drastically, as the incident magnetic field is gradually orthogonal to resistive surface and no longer produces an effective magnetic response. For the TM case illustrated in Fig. 5(d), the absorption rates and bandwidth decrease faster than in the case of TE wave. This is because the electric polariton that causes the resonant absorption in the composite structure can be effectively excited by the x component of the electric field. The y

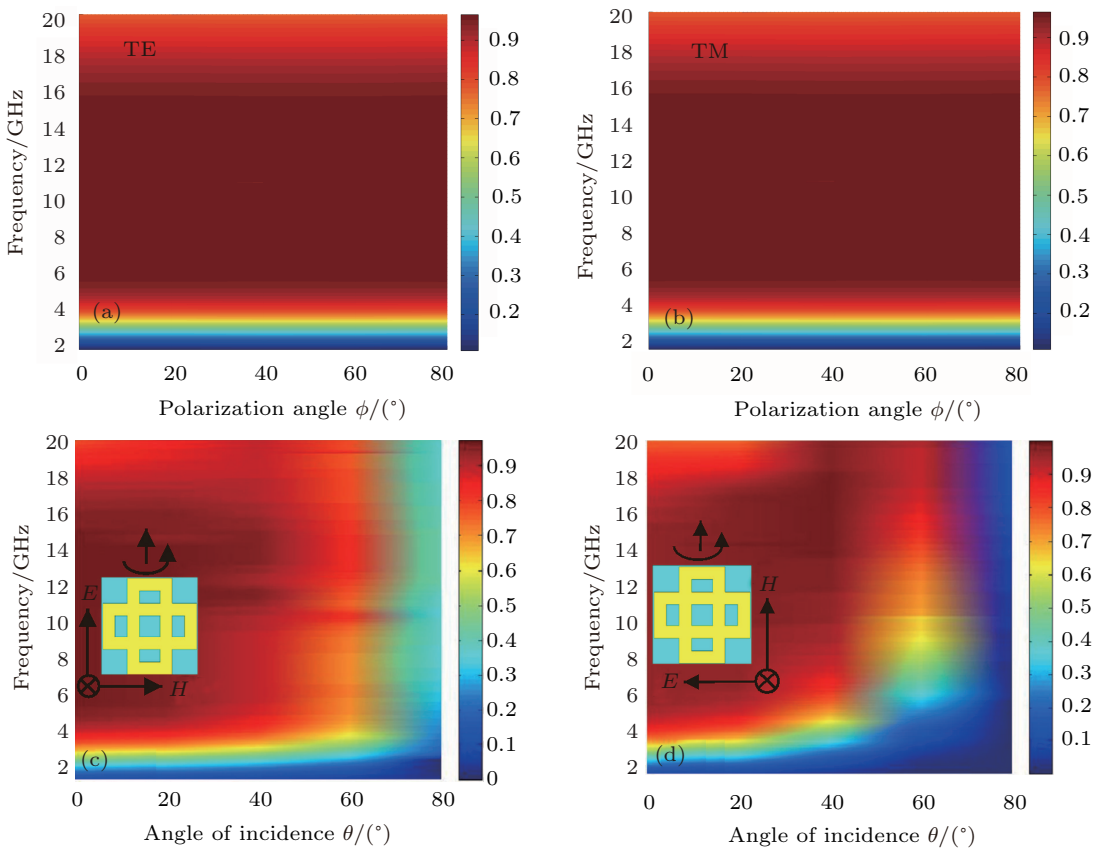


Fig. 5. (color online) Simulated absorption rates of this MA at different polarization angles for (a) TE and (b) TM waves. Simulated absorption rates of this MA at different angles of incidence for (c) TE and (d) TM waves.

component of the magnetic field contributes a little to the excitation of the electric polariton. Therefore, the x component of the electric field, which can efficiently drive resonance, will reduce gradually and the absorption band becomes narrower and narrower. Generally, these results demonstrate that the broadband MA could achieve high absorption rates at wide angles of incidence for both TE and TM waves.

3. Multi-reflection interference theory

To reveal absorbing property of the absorber quantitatively, the interference theory is involved to analyze the broadband absorption mechanism. For an uncoupled absorber model, the near-field coupling between layers is negligible, while introducing compensation sheets can cover the near-field coupling between layers for strong coupling structure.[5,17,19,22,23] The interference model of the structure and relevant variables are shown in Fig. 6. Assume that the copper film and resistive film layer are both kept to be zero thickness, but still retain the properties of their original structures.

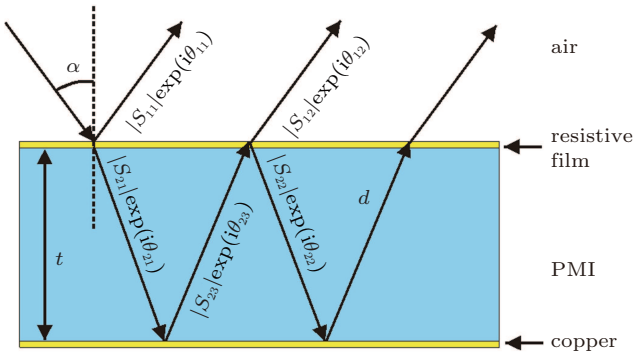


Fig. 6. (color online) Interference model of the MA and relevant variables.

Therefore, according to the interference theory,[5,19] the superposition of multiple reflections at interface 1 (resistive film) from air back to air can reach the overall reflection, thus

$$S_{11\,\mathrm{total}} = S_{11} - \frac{S_{12}S_{21}\,\mathrm{e}^{\mathrm{i}2\beta}}{1 + S_{22}\,\mathrm{e}^{\mathrm{i}2\beta}}, \tag{1}$$

where $\beta = kd$ is the propagation phase, k is the corresponding propagation wavenumber, $d = t/\cos\alpha$ is the propagation distance in PMI foam substrate, and α is the angle of incidence. The absorptivity can be reached from

$$A(\omega) = 1 - R(\omega) = 1 - |S_{11\mathrm{total}}|^2.$$

The reflection coefficients (S_{11}, S_{22}) and transmission coefficients (S_{12}, S_{21}) at the interface 1 are simulated by CST Microwave Studio.

As shown in Fig. 7, the copper film is removed during the simulation and the thickness values of air and substrate are both kept to be 9 mm.

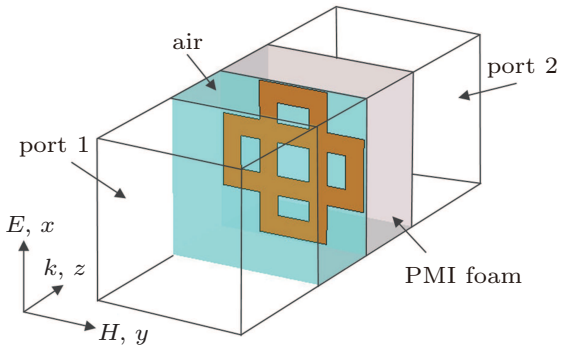


Fig. 7. (color online) Unit cell used to simulate S-parameters at interface 1.

Figure 8 shows the calculated reflectivity and absorption rate of the MA by using the interference model, which are in accordance with the simulated results.

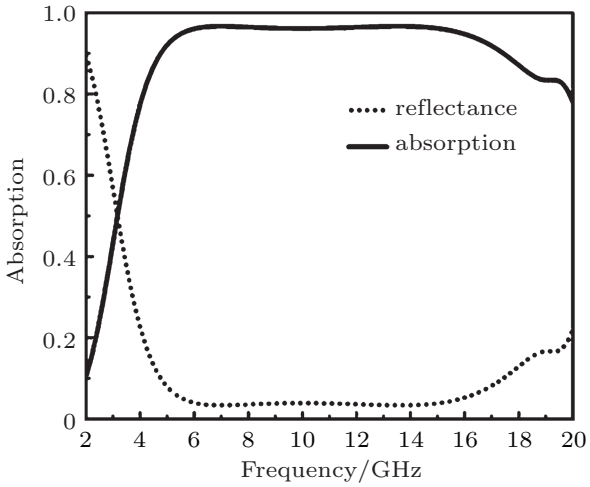


Fig. 8. Calculated reflection rate (short dot curve) and absorptivity (solid curve) by using the interference model.

Additionally, the absorption rates of the proposed absorber at oblique incidence and variable polarization angles are also investigated by using the interference theory. Figures 9(a) and 9(b) display the calculated absorption rates of the unit cell by using the interference model at different polarization angles for both TE and TM waves, respectively. According to the calculated results, the absorption rates for the absorber are acceptable compared with simulated results at wide polarization angles from 0° to 60° for both TE and TM modes. As the polarization angle further increases, the absorption band is split into several absorption frequency bands, which is caused by the characteristic of the theoretical model in which the coupling between the resistive film and the copper film is assumed to be ignored totally.[14]

The calculated absorption rates of the structure by using the interference model at different angles of incidence for TE and TM modes are shown in Figs. 9(c) and 9(d) respectively. These calculated absorption rates for the MA are in accordance with the simulated results approximately at wide angles of incidence from 0° to 60° for both TE and TM waves.

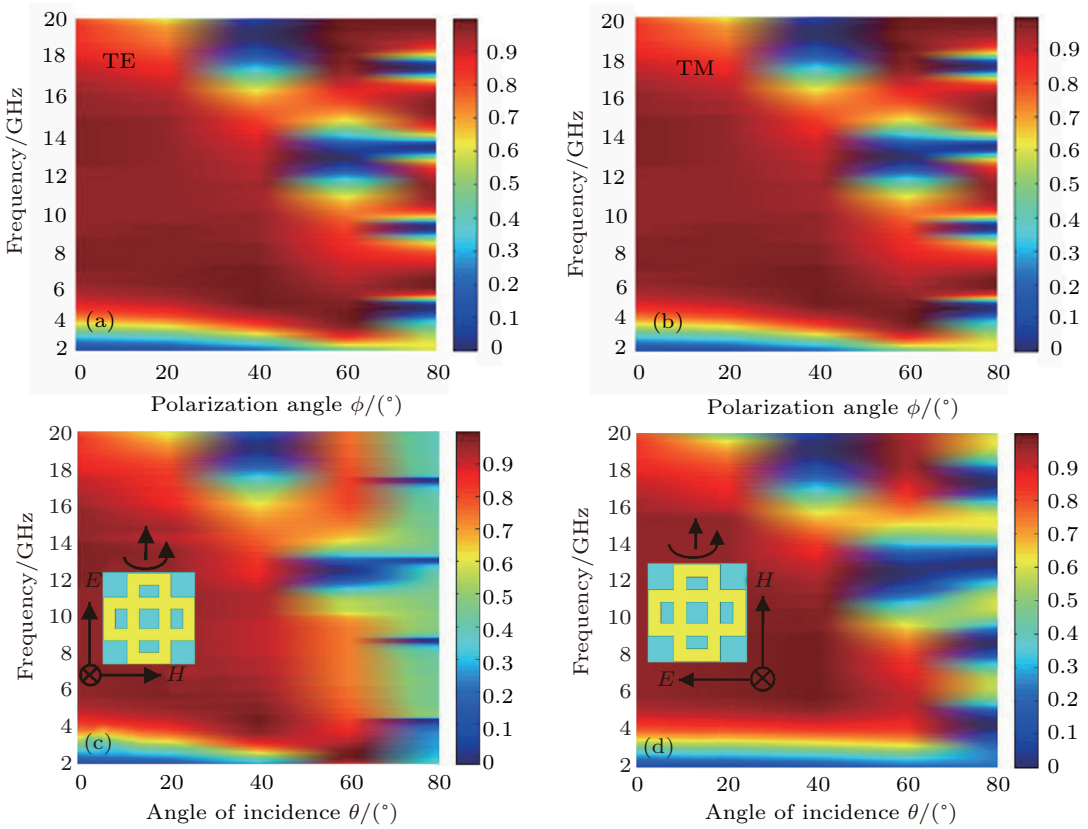


Fig. 9. (color online) Calculated absorptivities each as a function of frequency and polarization angle for (a) TE and (b) TM waves. Calculated absorptovities each as a function of frequency and angle of incidence for (c) TE and (d) TM waves.

4. Conclusions

In this work, we proposed a broadband, polarization-insensitive, and wide-angle MA based on resistive film, which exhibits absorption frequency band ranging from 4.75 GHz to 17.57 GHz with absorptivity above 90% at normal incidence. Distribution of surface power loss density indicates that the resistive film mainly supplies the broadband high absorption due to the ohmic loss. The MA can achieve polarization-insensitive absorption at the normal incidence and operate well at different angles of incidence for both TE and TM waves. The multi-reflection interference theory is adopted to quantitatively analyze the absorptions of the designed structure at different incidence angles and variable polarization angles for both TE and TM modes. Theoretical calculation and simulation results agree fairly well with each other at wide angles of incidence and wide polarization angles. Importantly, the proposed MA is also geometrically scalable. Therefore, our results are not limited to gigahertz frequencies and may be used in other parts of the electromagnetic spectrum. The designed MA has great promise for stealth technology and other relevant applications because of its broadband absorption and easy fabrication.

References

[1] Salisbury W W (U.S. Patent) 2 599 944 [1952-06-10]
[2] Knott E F and Langseth K B 1980 *IEEE Trans. Antennas Propag.* **28** 137
[3] Landy N I, Sajuyigbe S and Mock J J 2008 *Phys. Rev. Lett.* **100** 207402
[4] Landy N I, Bingham C M and Tyler T 2009 *Phys. Rev. B* **79** 125104
[5] Wang G D, Chen J F, Hu X W, Chen Z Q and Liu M H 2014 *Prog. Electromag. Res.* **145** 175
[6] Shi J X , Zhang W C, Xu W, Zhu Q, Jiang X, Li D D, Yan C C and Zhang D H 2015 *Chin. Phys. Lett.* **32** 094204
[7] Lee K T, Ji C G and Guo L J 2016 *Appl. Phys. Lett.* **108** 031107
[8] Sood D and Tripathi C C 2015 *Prog. Electromag. Res.* **44** 39
[9] Gu C, Qu S B, Pei Z B, Zhou H, Xu Z, Bai P, Peng W D and Lin B Q 2010 *Chin. Phys. Lett.* **27** 117802
[10] Cheng Y Z, Wang Y, Nie Y, Gong R Z, Xiong X and Wang X 2012 *J. Appl. Phys.* **111** 044902
[11] Yang G H, Liu X X, Lv Y L, Fu J H, Wu Q and Gu X M 2014 *J. Appl. Phys.* **115** 17E523
[12] Gu C, Qu S B, Pei Z B, Xu Z, Lin B Q, Zhou H, Bai P, Gu W, Peng W D and Ma H 2011 *Acta Phys. Sin.* **60** 087802 (in Chinese)
[13] Zhang H B, Zhou P H, Lu H P, Xu Y Q, Liang D F and Deng L J 2013 *IEEE Trans. Anten. Propag.* **61** 976
[14] Chen J F, Hu Z Y, Wang G D, Huang X T, Wang S M, Hu X W and Liu M H 2015 *IEEE Trans. Anten. Propag.* **63** 4367
[15] Wen Q Y, Xie Y S and Zhang H W 2009 *Opt. Express* **17** 20256
[16] Wen Q Y, Zhang H W and Xie Y S 2010 *Chin. J. Opt. Appl. Opt.* **3** 79 (in Chinese)
[17] Chen H T, Zhou J F, O'Hara J F, Chen F, Azad A K and Taylor A J 2010 *Phys. Rev. Lett.* **105** 073901
[18] Li H, Yuan L H, Zhou B, Shen X P, Cheng Q and Cui T J 2011 *J. Appl. Phys.* **110** 014909
[19] Chen H T 2012 *Opt. Express* **20** 7165
[20] Shen X P, Yang Y, Zang Y Z, Gu J Q, Han J G, Zhang W L and Cui T J 2012 *Appl. Phys. Lett.* **101** 154102
[21] Wang G D, Liu M H, Hu X W, Kong L H, Cheng L L and Chen Z Q 2014 *Chin. Phys. B* **23** 017802
[22] Huang L, Chowdhury D R, Ramani S, Reiten M T, Luo S N, Azad A K, Taylor A J and Chen H T 2012 *Appl. Phys. Lett.* **101** 101102
[23] Wang H T, Chen W, Huang Y and Wen G 2013 *AIP Adv.* **3** 102118